RESEARCH ARTICLE

FASEB BioAdvances WILEY

Comprehensive analysis of circRNAs for N7-methylguanosine methylation modification in human oral squamous cell carcinoma

Dongyuan Sun[1,2] | Ning Song[1] | Minmin Li[1] | Xi Chen[1] | Xinyue Zhang[1] |
Yang Yu[1,2] | Jicheng Ying[1] | Mengqi Xu[1] | Wentian Zheng[1] | Chengbing Han[3] |
Honghai Ji[1,2] | Yingying Jiang[1,2]

[1]School of Stomatology, Weifang Medical University, Weifang, China

[2]Department of Stomatology, Affiliated Hospital of Weifang Medical University, Weifang, China

[3]Department of Stomatology, First Affiliated Hospital of Weifang Medical University, Weifang, China

Correspondence
Yingying Jiang and Honghai Ji, School of Stomatology, Weifang Medical University, 7166, Bao Tong West Street, Weifang 261053, China.
Email: jiangyy@wfmc.edu.cn and 13053611122@163.com

Abstract

N7-methylguanosine (m7G) modification is closely related to the occurrence of tumors. However, the m7G modification of circRNAs in oral squamous cell carcinoma (OSCC) remains to be investigated. Methylated RNA immunoprecipitation sequencing (MeRIP-seq) was used to measure the methylation levels of m7G and identify m7G sites in circRNAs in human OSCC and normal tissues. The host genes of differentially methylated and differentially expressed circRNAs were analyzed by Gene Ontology (GO) enrichment and Kyoto Encyclopedia of Genes and Genomes (KEGG) pathway analyses, and circRNA–miRNA–mRNA networks were predicted using the miRanda and miRDB databases. The analysis identified 2348 m7G peaks in 624 circRNAs in OSCC tissues. In addition, the source of m7G-methylated circRNAs in OSCC was mainly the sense overlap region compared with normal tissues. The most conserved m7G motif in OSCC tissues was CCUGU, whereas the most conserved motif in normal tissues was RCCUG (R=G/A). Importantly, GO enrichment and KEGG pathway analysis showed that the host genes of differentially methylated and differentially expressed circRNAs were involved in many cellular biological functions. Furthermore, the significantly differentially expressed circRNAs were analyzed to predict the circRNA–miRNA–mRNA networks. This study revealed the whole

profile of circRNAs of differential m7G methylation in OSCC and suggests that m7G-modified circRNAs may impact the development of OSCC.

KEYWORDS

circular RNA, methylated RNA immunoprecipitation sequencing (MeRIP-seq), N7-methylguanosine (m7G), oral squamous cell carcinoma (OSCC), RNA methylation

1 | INTRODUCTION

Oral squamous cell carcinoma (OSCC) is a common type of head and neck squamous cell carcinoma (HNSCC), and at least 90% of oral cancers are squamous cell carcinomas.[1] Patients with OSCC have a 5-year survival rate of less than 50%[2] and high recurrence and metastasis rates.[3] According to the latest statistics, there were 377,000 cases of OSCC and 177,000 deaths worldwide in 2020.[4] In addition, most patients are usually at an advanced stage when the disease is discovered, which seriously affects the quality of their survival.[5] Therefore, it is important to investigate the mechanisms of OSCC pathogenesis.

Non-coding RNAs (ncRNAs) include long noncoding RNAs (lncRNAs), small nucleolar RNAs (snoRNAs), microRNAs (miRNAs), and circular RNAs (circRNAs).[6] CircRNAs are a class of ncRNA molecules that do not have a 5′ terminal cap or a 3′ terminal poly (A) tail and are covalently bonded to form a closed loop structure.[7-9] CircRNAs can affect proliferation, invasion and metastasis in OSCC.[10,11] Moreover, circRNAs are important regulators of cancer development that can function as transcription regulators, decoys to sponge miRNAs, and scaffolds for protein–protein interactions and interact with RNA-binding proteins (RBPs).[12-16] For instance, circRNA_100290 regulates the expression of CDK6 through the sponge absorption of miRNA-29b, thus promoting the proliferation of oral cancer.[17] Studies have found that circ_0000140 can bind to miR-31 and upregulate its target gene, LATS2, affecting epithelial-mesenchymal transition (EMT) in OSCC cells.[18] However, the role of circRNAs in OSCC has not been fully elucidated, and further studies are needed.

RNA methylation, which is one of the most common post-transcriptional modifications, refers to the addition of a methyl group to RNA molecules after their transcription from DNA.[19] RNA methylation plays an important role in transcriptional regulation and includes N6-methyladenosine (m6A), 5-methylcytidine (m5C), N7-methylguanosine (m7G) and so on.[20,21] Recently, m7G methylation, originally considered as messenger RNA (mRNA) 5′ caps modifications, has been detected at defined internal positions within multiple types of RNAs, including transfer RNAs (tRNAs), ribosomal RNAs (rRNAs), miRNAs, lncRNAs and mRNAs by methylated RNA immunoprecipitation sequencing (MeRIP-seq),[22-26] which often affects the processing and maturation of some ncRNAs, ultimately affecting protein synthesis.[27] Chen et al. reported that the m7G methyltransferase-like 1 (METTL1) promotes m7G modification of tRNA, facilitating the translation of many vital oncogenes in HNSCC.[28] Numerous studies have confirmed that m6A is common in circRNAs and that circRNAs influence disease progression via methylation regulation.[29] However, the underlying mechanism of m7G-circRNAs is unknown[30] and few studies have investigated the role of circRNAs and methylation in regulating the occurrence and development of oral cancer.[29] The exploration of m7G-circRNAs is conducive to further elucidation of the pathogenic mechanisms in OSCC.

Through a comprehensive analysis of the m7G characteristics of circRNA, this study found significant differences in the m7G modification level of circRNAs and the expression of circRNAs between OSCC and normal tissues. The m7G peak length and the source of m7G-modified circRNAs also differed between OSCC tissues and normal tissues. Furthermore, Gene Ontology (GO) and Kyoto Encyclopedia of Genes and Genomes (KEGG) analysis showed that different circRNA methylation and expression levels were associated with different biological functions. Furthermore, the significantly different circRNAs were analyzed to predict the circRNA–miRNA–mRNA networks. In general, a comprehensive analysis of circRNAs for m7G methylation modification can provide research value for future studies on the role of m7G in OSCC.

2 | MATERIALS AND METHODS

2.1 | Tissue collection and RNA preparation

Six tissue samples from three OSCC patients were collected from the Department of Stomatology of the First Affiliated Hospital of Weifang Medical University in this study. The study was conducted according to the guidelines of the Declaration of Helsinki, and approved by the Ethics

Committee of Weifang Medical University. Informed consent was obtained from all the subjects. Tissue with a diameter of 0.5–1 cm was taken from the center of the patient's OSCC tissue. Paired normal tissue of similar size was obtained from the patient at a distance of more than 2 cm from the OSCC tissue edge. The samples were collected, rinsed with saline, and rapidly cryopreserved in liquid nitrogen. The tissues were stained with hematoxylin-eosin (HE) and confirmed by the professional pathologists. No patients had received preoperative radiation therapy or chemotherapy. Total RNA extraction was provided by Cloud-seq Biotech Inc (Shanghai, China). A NanoDrop ND-1000 instrument (Thermo Fisher Scientific) was used to measure the RNA concentration of each sample, and the OD 260/280 values of 1.8–2.1 were considered to ensure good RNA purity (Table 1).

2.2 | RNA library preparation and sequencing

CloudSeq Inc. (Shanghai, China) provided the high-throughput RNA sequencing service. rRNAs from total RNA were removed with the GenSeq® rRNA Removal Kit (GenSeq, Inc.) kit. After rRNAs removal, the samples were utilized to construct RNA sequencing libraries using the GenSeq® Low Input Whole RNA Library Prep Kit (GenSeq, Inc.). The constructed sequencing library was subjected to quality control and quantified with the BioAnalyzer 2100 system (Agilent Technologies, Inc.), high-throughput sequencing of the library was controlled using an Illumina NovaSeq 6000 instrument with 150 bp paired-end reads.

2.3 | MeRIP library preparation and sequencing

CloudSeq Inc. (Shanghai, China) provided the m7G-MeRIP-seq service. The rRNAs from total RNA were removed with the GenSeq® rRNA Removal Kit (GenSeq, Inc.) kit. The 5′-cap was removed from the total RNA using

an mRNA decapping enzyme (New England Biolabs). Immunoprecipitation (IP) was then performed with the GenSeq®m7G-IP kit (GenSeq Inc.). Briefly, after rRNAs removal, the decapped RNA was processed into fragments of approximately 200 nt using the fragmentation reagent supplied in the kit. Protein A/G magnetic beads and m7G antibody (RN017M, MBL) were rotated and incubated at room temperature for 1 h to bind the antibody to the magnetic beads. The RNA fragments and the antibody coupled with magnetic beads were then rotated at 4°C and incubated for 4 h to bind the RNA to the antibody. After incubation, the RNA/antibody complexes were washed several times, and the captured RNA was then eluted from the complexes and purified. The RNA libraries for IP and input samples were constructed using the GenSeq® Low Input Whole RNA Library Prep Kit (GenSeq, Inc.). The constructed library was subjected to quality control with an Agilent 2100 bioanalyzer, and high-throughput sequencing was then performed on the NovaSeq platform (Illumina; Figure 1A).

2.4 | Identification and analysis of the host genes of differentially expressed circRNAs

Paired-end reads were subjected to quality control based on Q30 after harvesting with an Illumina NovaSeq 6000 instrument. Cutadapt software[31] (v1.9.3) was used to delete 3′ adaptor trimming and low-quality reads. Then, STAR software[32] (v2.5.1b) was used to align the high-quality reads to the reference genome/transcriptome. After the detection and identification of circRNAs using DCC software[33] (v0.4.4), the circBase database (http://www.circbase.org/)[34] and the Circ2Traits database (http://gyanxet-beta.com/circdb/)[35] were used to annotate the identified circRNAs. Data normalization and differentially expressed circRNA screening were performed using edgeR software[36] (v3.16.5). A p value ≤ 0.05 and fold change ≥ 2.0 were used as the thresholds to screen the upregulated or downregulated circRNAs.

TABLE 1 Detailed data on the quality of RNA obtained by NanoDrop ND-1000.

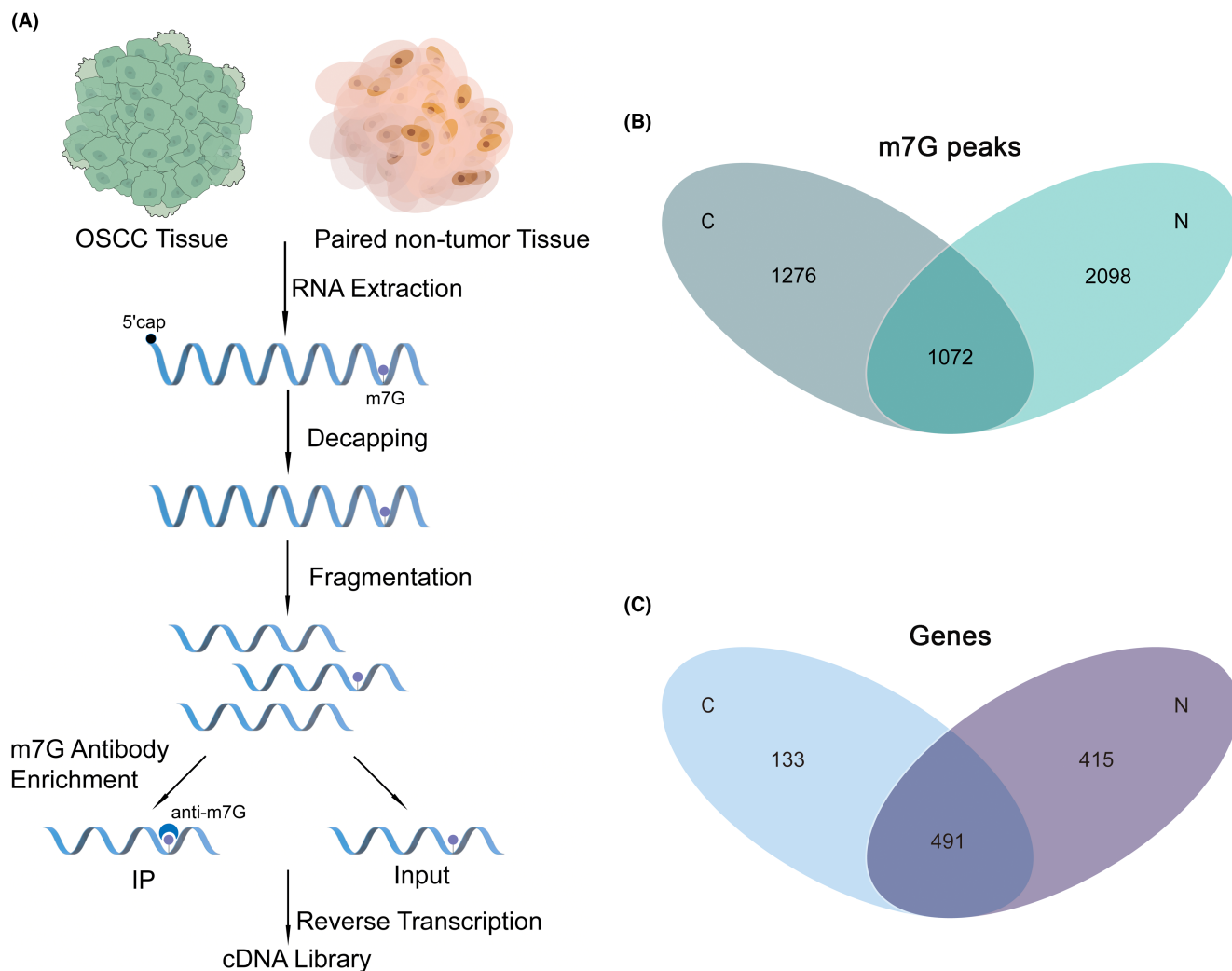| Patient ID	Sample	OD 260/280 ratio	Conc. (ng/μL)	Volume (μL)	Quantity (μg)	Q30 (%)
1	OSCC	1.83	1254.64	18	22.58	92.40
2	OSCC	1.85	1544.31	18	27.80	92.53
3	OSCC	1.83	1445.83	18	26.02	92.84
1	Paired nontumor	1.81	1319.98	18	23.76	89.77
2	Paired nontumor	1.87	600.68	18	10.81	92.39
3	Paired nontumor	1.88	1112.59	18	20.03	90.17

(A)

(B)

(C)

FIGURE 1 Flow chart of the methylated RNA immunoprecipitation sequencing (MeRIP-seq) experiment and m7G methylation distribution characteristics. (A) After the extracted RNA was fragmented, the 5′-cap was removed; one group subsequently pulled down the m7G-rich RNA fragment with m7G-antibody enrichment, and another group was used as input. (B) Venn diagram of m7G peaks identified in circRNAs in OSCC and normal tissues. (C) Venn diagram of m7G target genes in OSCC and normal tissues. C, cancer; N, normal.

2.5 | Identification and analysis of the host genes of differentially methylated circRNAs

Raw reads (raw data) were generated after sequencing with an Illumina NovaSeq 6000 instrument, image analysis, and base identification. First, quality control was achieved based on Q30, and Q30 > 80% indicated high sequencing quality. Cutadapt software (v1.9.3) was used to separate high-quality clean reads and delete low-quality reads. The clean reads of the input libraries were aligned to the reference genome using STAR software[32] (v2.5.1b), and circRNA identification was then performed by DCC software[33] (v0.4.4) using the STAR alignment results. The clean reads of all libraries were then aligned to the reference genome using Hisat2 software[37] (v2.0.4). The

methylation sites in each sample were identified using MACS software[38] with default parameters. Differentially methylated sites were recognized using diffReps software[39] ($p \leq 0.00001$ and fold change ≥ 2.0).

2.6 | GO and KEGG analysis

The host genes of differentially methylated and differentially expressed circRNAs were analyzed by GO enrichment analysis; the results were related to molecular function (MF), biological process (BP), and cellular component (CC), and GO terms with $p \leq 0.05$ were considered to indicate that the enrichment results were reliable. We also performed KEGG pathway analysis of these host genes. We presented molecular data from genomics, transcriptomics, proteomics, and

metabolomics on KEGG pathway maps to infer their biological functions. A $p \leq 0.05$ represented a significant difference.

2.7 | Prediction and analysis of the circRNA–miRNA–mRNA interaction network

Competitive endogenous RNA (ceRNA) refers to the ability of molecules (mRNA, lncRNA, circRNA, etc) to compete to bind the same miRNA through the miRNA response element to regulate each other's expression levels.[40,41] And ceRNA networks can link the function of protein-coding mRNAs with that of ncRNAs. We predicted the circRNA–miRNA–mRNA ceRNA networks by miRanda[42] and the miRDB database (http://mirdb.org).[43] The circRNA–miRNA–mRNA networks were mapped using Cytoscape software[44] (v3.8.0).

2.8 | Statistical analysis of m7G data

The peak sequences of m7G methylation (50 bp on each side of the midpoint) in each group were scanned with Dreme[45] software. Based on the results obtained, the motif with the smallest E value was selected to be the most significant. The E value was obtained by multiplying the enrichment p value by the number of candidate patterns tested. Fisher's exact test was used to calculate the enrichment p value of the motifs in the positive sequences. We used GraphPad Prism 7.0 to graph the data and SPSS 26.0 for the statistical analyses. The length of the peaks between the two groups were compared by a t test (two-sample). A $p < 0.05$ was considered to indicate a significant difference.

3 | RESULTS

3.1 | General characteristics of m7G methylation in OSCC and normal tissues

The analysis identified 2348 m7G peaks in OSCC tissues, whereas 3170 m7G peaks were detected in normal tissues (Figure 1B). We also mapped 624 m7G-modified genes in OSCC tissues and 906 annotated genes in normal tissues, respectively (Figure 1C). Compared to normal tissues, 1276 unique peaks and 133 unique m7G-modified genes were identified in OSCC tissues. Among them, 1072 peaks and 491 annotated genes were identified both in OSCC tissues and normal tissues. On average, there were approximately 9.59 m7G methylation peaks per unique gene in OSCC tissues and approximately 5.05 m7G methylation peaks per unique gene in normal tissues.

3.2 | Characteristic analysis of the m7G peak length on circRNAs

To investigate the characteristics of the m7G peaks on circRNAs in OSCC tissues, we analyzed the length of the methylation RNA sites in OSCC and normal tissues. A significant difference was found between OSCC and normal tissues ($p < 0.0001$), and the mean length in OSCC and normal tissues was 477.7 and 338.6 bp, respectively (Figure 2A).

3.3 | Characterization of the distribution of m7G methylation sites on chromosomes

We visualized the m7G site distribution characteristics of circRNAs on each chromosome corresponding to OSCC and normal tissues using the RCircos package. The results showed that the distribution of m7G modification sites on circRNAs in OSCC tissues was different from that in normal tissues. Compared with autosomes, sex chromosomes had little distribution of m7G methylation sites (Figure 2B).

3.4 | Analysis on the source of m7G-methylated circRNAs in OSCC and normal tissues

The analysis of the source data of each methylated circRNA showed that the ratio of m7G-modified circRNA classified according to the source region differed between the two types of tissues and we plotted pie charts to analyze the corresponding composition in OSCC and normal tissues (Figure 2C,D). Most m7G-modified circRNAs in OSCC tissues were derived from the sense overlapping regions (Cancer:65.67%, Normal:59.18%). The source ratio of m7G-methylated circRNAs derived from exonic regions in OSCC tissues was less than that in normal tissues (Cancer: 21.73%, Normal: 28.08%). The source of m7G-methylated circRNAs derived from intronic regions (Cancer: 10.34%, Normal: 10.50%), antisense regions (Cancer: 1.99%, Normal: 2.09%) and intergenic regions (Cancer: 0.27%, Normal: 0.15%) showed almost no difference between the two groups.

3.5 | Motif analysis of m7G methylation sites

The m7G methylation peaks were analyzed using Dreme software to obtain motifs. We found that the most conserved m7G motif in OSCC tissues was CCUGU with a p value of 2.0e-007 and an E value of 1.0e-002, whereas

(A)

(B)

OSCC
Normal

(C) Cancer

0.27%
10.34%
21.73%
1.99%
65.67%

intronic sense overlapping antisense exonic intergenic

(D) Normal

0.15%
10.50%
28.08%
2.09%
59.18%

intronic sense overlapping antisense exonic intergenic

(E) Cancer

P-value:2.0e-007
E-value:1.0e-002

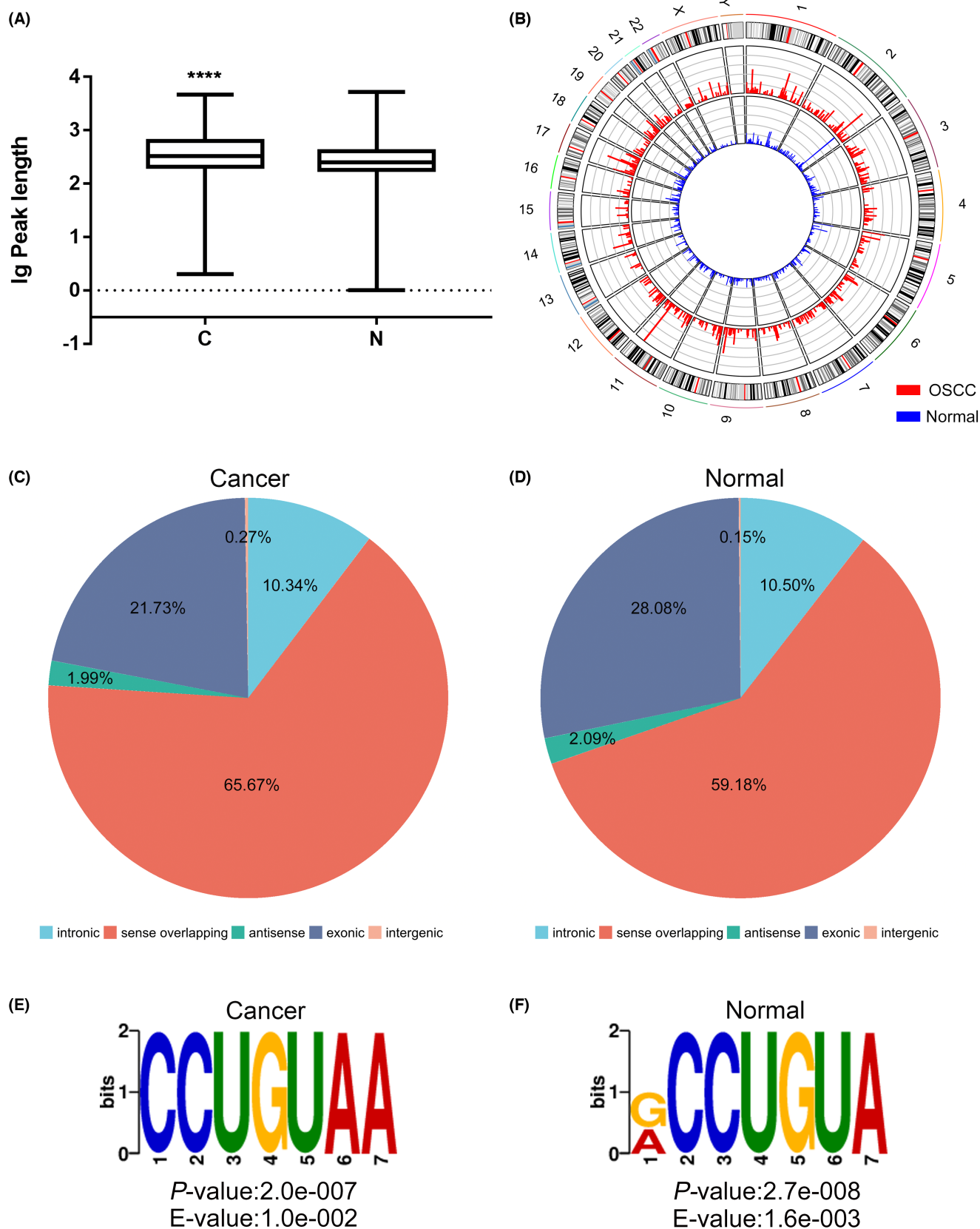**(F)** Normal

P-value:2.7e-008
E-value:1.6e-003

FIGURE 2 Common features of m7G-modified circRNAs in OSCC tissues. (A) Comparison of the width of m7G peaks in OSCC and normal tissues. C: cancer; N: normal. ****$p < 0.0001$ (B) Visualization of chromosomes in OSCC and normal tissues. (C, D) Pie chart of the source composition of m7G-modified circRNA classified according to the source region in OSCC and normal tissues. (E, F) Most representative motifs in OSCC and normal tissues, respectively.

the most conserved motif in normal tissues was RCCUG (R=G/A), with a *p* value of 2.7e-008 and an *E* value of 1.6e-003 (Figure 2E,F). The results suggested that the motif with similar sequence may be necessary for m7G methylation in both types of tissues.

3.6 | GO analysis

To investigate the function of host genes of differentially methylated circRNAs in OSCC, we performed GO analysis of those host genes based on BP, CC, and MF. For host genes with upregulated m7G-methylated circRNAs in OSCC, GO analysis revealed that those genes were enriched in antigen processing and presentation of endogenous peptide antigen

via MHC class, antigen processing and antigen presentation of endogenous peptide antigen, and cellular response to prostaglandin E stimulus (GO term: BP), intracellular, cytoskeleton, and cytosol (GO term: CC), peptide antigen binding, cytoskeletal protein binding, and damaged DNA binding (GO term: MF; Figure 3A). Genes with downregulated m7G-methylated circRNAs in OSCC were associated with antigen processing and presentation of endogenous peptide antigen via MHC class I, antigen processing and presentation of endogenous peptide antigen and antigen processing and presentation of endogenous antigen (GO term: BP), intracellular, cytoplasm, and MHC protein complex (GO term: CC), peptide antigen binding, protein N-terminus binding, and cytoskeletal protein binding (GO term: MF; Figure 3C).
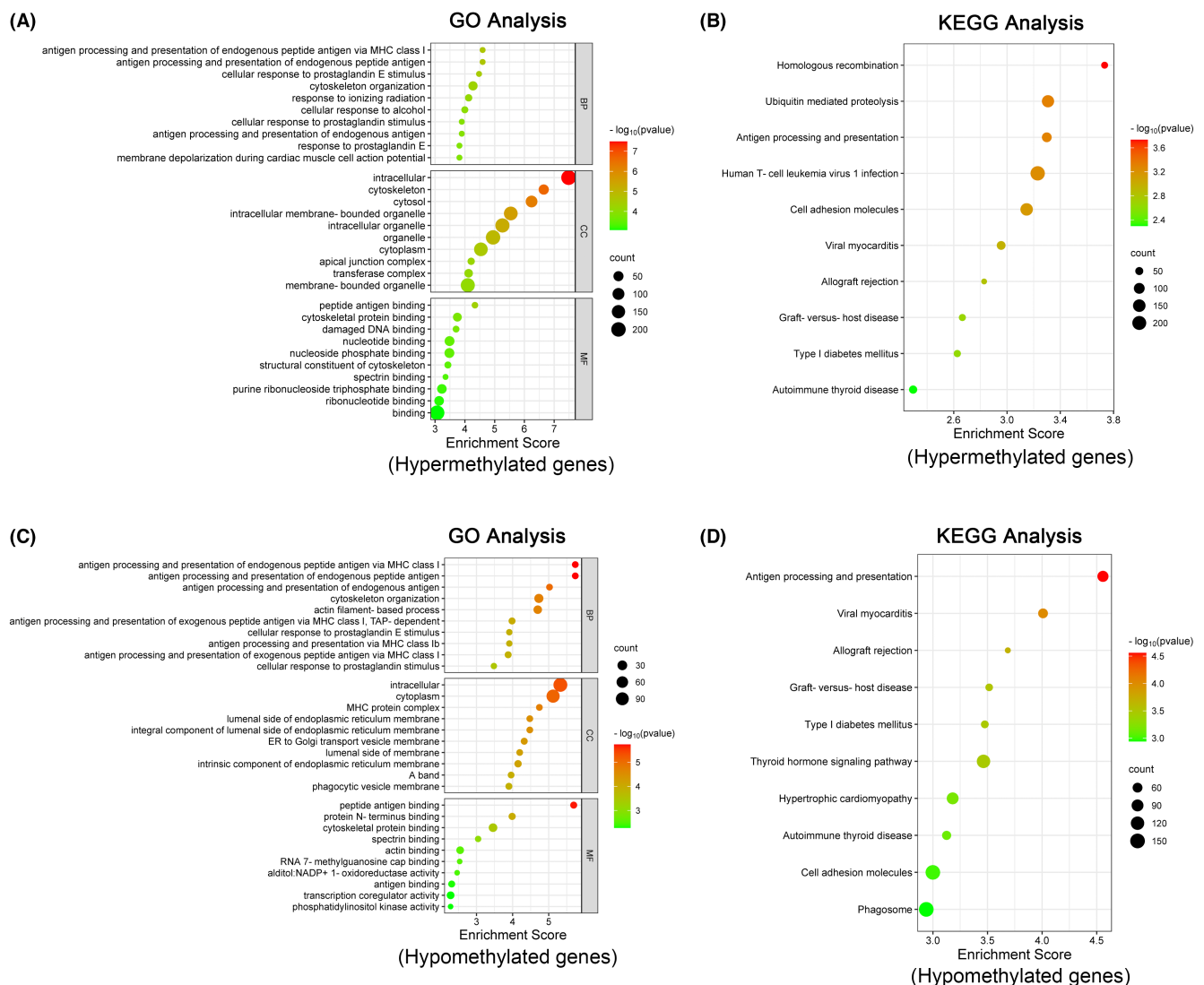

FIGURE 3 GO enrichment and KEGG pathway analysis of host genes of differentially methylated circRNAs. (A) GO enrichment analysis of host genes of upregulated m7G circRNAs in OSCC, including: biological process (BP), cellular component (CC), and molecular function (MF) analysis. (B) KEGG pathway analysis of host genes of upregulated m7G circRNAs in OSCC. (C) GO enrichment analysis of host genes of downregulated m7G circRNAs in OSCC, including: biological process (BP), cellular component (CC), and molecular function (MF) analysis. (D) KEGG pathway analysis of host genes of downregulated m7G circRNAs in OSCC.

To explore the impact of circRNA expression in OSCC tissues, we performed GO analyses on genes with upregulated and downregulated circRNA expression. GO analysis revealed that genes with upregulated circRNA expression in OSCC were mainly associated with cellular response to radiation, regulation of double-strand break repair via homologous recombination, and mRNA processing (GO term: BP), nuclear chromosome, chromosome, and nuclear chromatin (GO term: CC), bHLH transcription factor binding, chromatin binding, and RNA polymerase II transcription factor binding (GO term: MF; Figure 4A). Genes with downregulated circRNA expression were mainly related to cardiac muscle cell development, cardiac cell development, and cardiac muscle cell differentiation

(GO term: BP), condensed nuclear chromosome, nuclear lumen, and nucleus (GO term: CC), structural constituent of muscle, cytoskeletal protein binding, and DNA-dependent ATPase activity (GO term: MF; Figure 4C).

3.7 | KEGG analysis

According to the KEGG pathway analysis, genes with upregulated m7G-methylated circRNAs in OSCC tissues were associated with homologous recombination, ubiquitin-mediated proteolysis, and antigen processing and presentation pathways (Figure 3B), whereas those with downregulated m7G-methylated circRNAs were
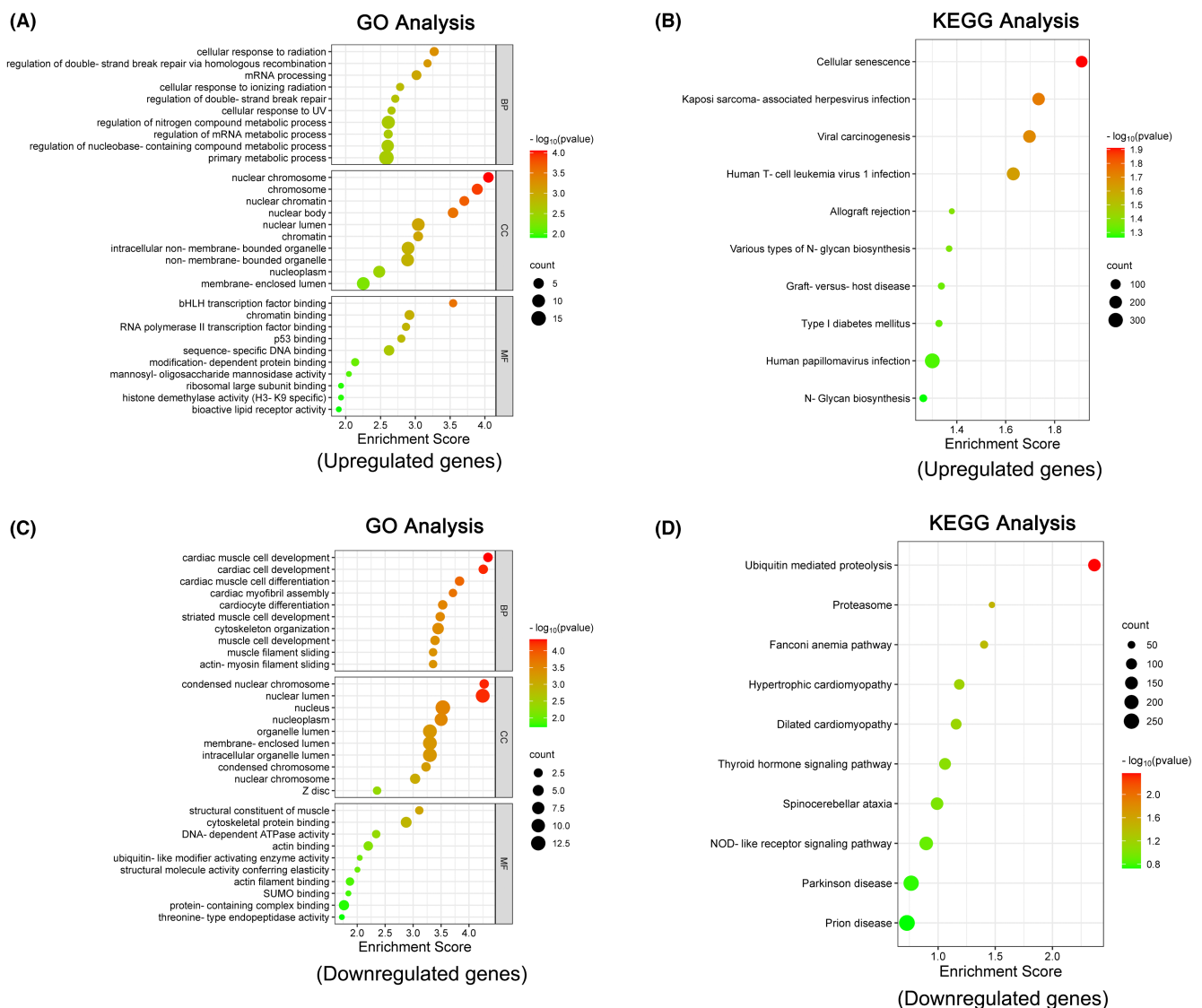

FIGURE 4 GO enrichment and KEGG pathway analysis of host genes of differentially expressed circRNAs. (A) GO enrichment analysis of host genes with upregulated circRNAs in OSCC, including: biological process (BP), cellular component (CC), and molecular function (MF) analysis. (B) KEGG pathway analysis of host genes with upregulated circRNAs in OSCC. (C) GO enrichment analysis of host genes with downregulated circRNAs in OSCC, including: biological process (BP), cellular component (CC), and molecular function (MF) analysis. (D) KEGG pathway analysis of host genes with downregulated circRNAs in OSCC.

TABLE 2 Top 10 upregulated methylated peaks.

chrom	txStart	txEnd	GeneName	Foldchange
chr12	53121321	53121800	KRT4	941.3
chr11	102338901	102339380	MMP7	701
chr11	102326821	102327200	MMP7	700.9
chr17	39708641	39709300	KRT9	591
chr1	744741	745100	RP11-206L10.9	567.8
chr17	43594861	43595080	LRRC37A4P	564.6
chr2	210989581	210989960	KANSL1L	532.1
chr1	111695101	111695340	CEPT1	532.1
chr3	170088921	170089300	SKIL	509.8
chr3	176671341	176671780	G058758	500.6

TABLE 3 Top 10 downregulated methylated peaks.

chrom	txStart	txEnd	Gene name	Foldchange
chr15	32796421	32796640	WHAMMP1	908.5
chr2	24799261	24799540	NCOA1	516.3
chr16	1447541	1448140	UNKL	418.6
chr9	129788921	129789260	RALGPS1	283.9
chr9	110075361	110075560	RAD23B	206.7
chr1	91390201	91390480	ZNF644	177.8
chr17	10370021	10370280	MYH1	172.4
chr5	79024737	79024840	CMYA5	159.58272
chr7	130636201	130636400	LINC-PINT	138.8
chr7	158591721	158591763	ESYT2	138.08219

associated with antigen processing and presentation, viral myocarditis, and allograft rejection pathways (Figure 3D).

The results from the KEGG analysis revealed that genes with upregulated circRNA expression were involved in the cellular senescence, Kaposi sarcoma-associated herpesvirus infection, and viral carcinogenesis pathways (Figure 4B), and that genes with downregulated circRNA expression were involved in the ubiquitin-mediated proteolysis, proteasome, and Fanconi anemia pathways (Figure 4D).

3.8 | Differences in m7G peaks between OSCC and normal tissues

We analyzed the differences in m7G peaks between the two sets of OSCC and normal tissues. The analysis of different methylation sites revealed 860 upregulated peaks and 211 downregulated peaks in OSCC tissues ($p \leq 0.00001$ and fold change ≥ 2.0). From these peaks, we have selected and listed the top 10 methylation peaks (upregulation and downregulation) with the largest fold change values in Tables 2 and 3, respectively. We selected circRNAs with upregulated m7G-methylated peak (chr3:170079046-170099129, chr1:111690501-111724893) and downregulated m7G-methylated peak (chr2:24799260-24799540,

chr1:91390201-91390480), and the corresponding methylation sites were visualized using Integrative Genomics Viewer (IGV) software (v2.14.1; Figure 5A–D).

3.9 | Differential expression of circRNAs in OSCC and normal tissues

The heatmap2 package of R was used to perform a clustering analysis to identify differential circRNA expression profiling with normalized reads, and the heatmap showed the differential expression of circRNAs in OSCC and normal tissues (Figure 6A). The volcano (Figure 6B) and scatter plots (Figure 6C) showed that a total of 17 circRNAs had elevated expression and 21 circRNAs had reduced expression in OSCC tissues. From these circRNAs, we selected the top 10 circRNAs with elevated and decreased expression with the most significant fold change values in Tables 4 and 5, respectively. In our study, we screened the top three upregulated circRNAs (chr8:48192450-48206619, chr17:28180406-28182248 and chr10:116590611-116608496) and the top three downregulated circRNAs (chr3:99567139-99569914, chr2:179516028-179516243 and chr2:24357989-24369956) in OSCC tissues. The ceRNA network consisted of the top

five miRNAs bound to the screened circRNAs and the top five mRNAs bound to the miRNAs. Furthermore, the network map included six differentially expressed circRNAs, 30 miRNAs, and 142 mRNAs (Figure 6D,E).

3.10 | Conjoint analysis of m7G methylation and circRNA expression

The relationship between the differentially m7G-modified circRNAs and the corresponding circRNA expression

levels was analyzed by combining MeRIP-seq and RNA sequencing data. The intersection of differentially methylated peaks and differentially expressed circRNAs was obtained. The results showed that 2 downregulated circRNAs with hypermethylation (chr1:169947226-170001116, chr1:35559515-35578782) derived from sense overlap region of KIFAP3 and ZMYM1 respectively and 1 downregulated circRNA with hypomethylation (chr12:116668338-116675510) derived from sense overlap region of MED13L were found. We predicted the circRNA–miRNA–mRNA network map of these three circRNAs,
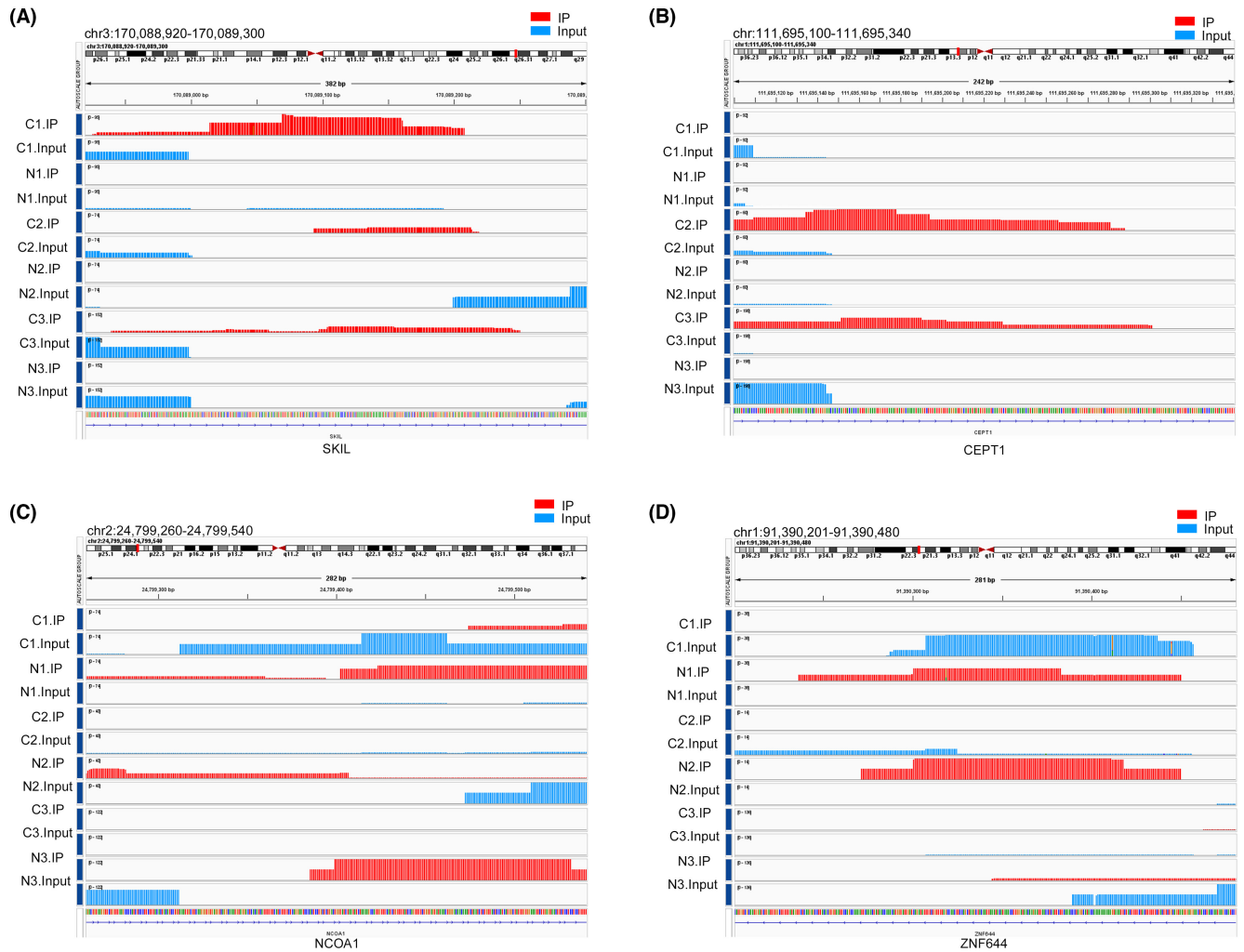

FIGURE 5 Visualization of methylation peaks on differential m7G methylation modifies circRNAs in OSCC tissues. (A) Methylation peaks of circRNA "chr3:170079046-170099129" at the locus (Start: 170088920; End: 170089300). (B) Methylation peaks of circRNA "chr1:111690501-111724893" at the locus (Start: 111695100; End: 111695340). (C) Methylation peaks of circRNA "chr2: 24799260-24799540" at the locus (Start: 24799260; End: 24799540). (D) Methylation peaks of circRNA "chr1: 91390201-91390480" at the locus (Start: 91390201; End: 91390480).

FIGURE 6 Analysis of circRNA differential expression in OSCC tissues. (A) Heatmap of cluster analysis of circRNA expression in OSCC and normal tissues. (B) Volcano plot of circRNA expression in OSCC tissues compared to normal tissues. (C) Scatter plot of circRNA expression in OSCC tissues compared to normal tissues. C, cancer; N, normal. (D) The circRNA–miRNA–mRNA network of the top three upregulated circRNAs (chr8:48192450-48206619, chr17:28180406-28182248 and chr10:116590611-116608496). (E) The circRNA–miRNA–mRNA network of the top three downregulated circRNAs (chr3:99567139-99569914, chr2:179516028-179516243, and chr2:24357989-24369956) and their target miRNAs and mRNAs (Top five miRNAs and mRNAs are shown on the map).
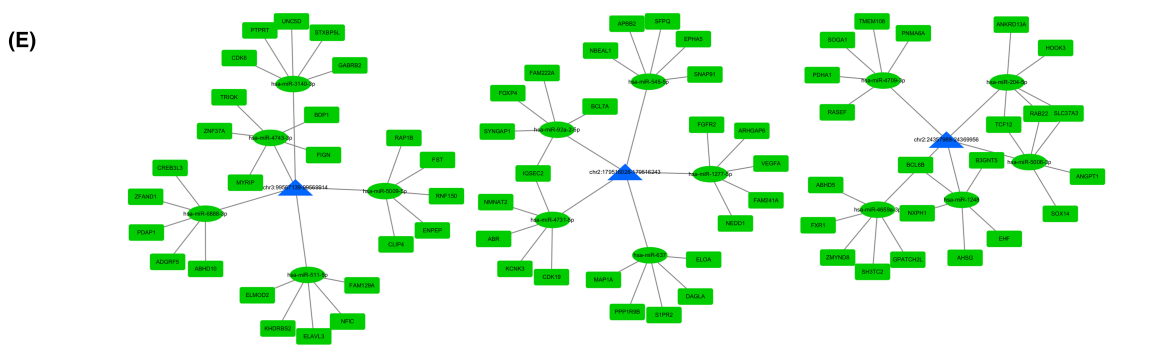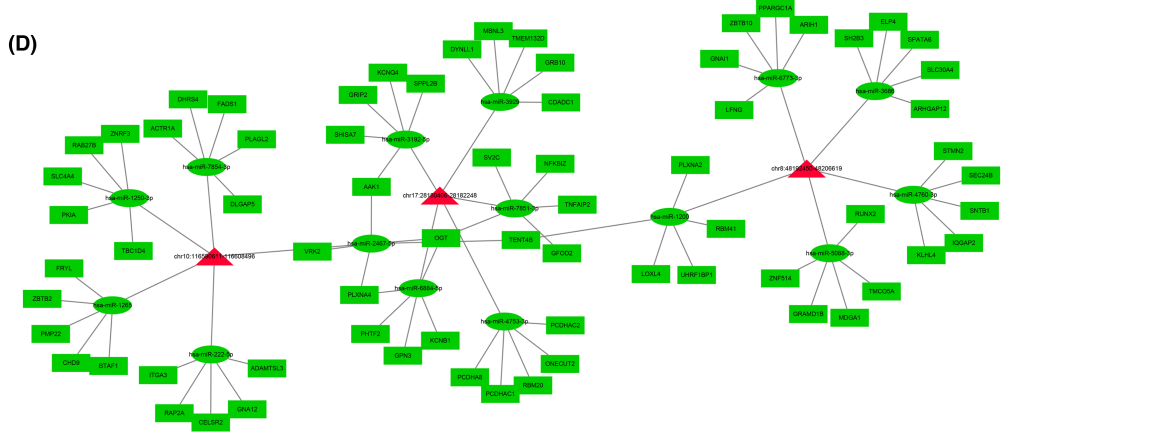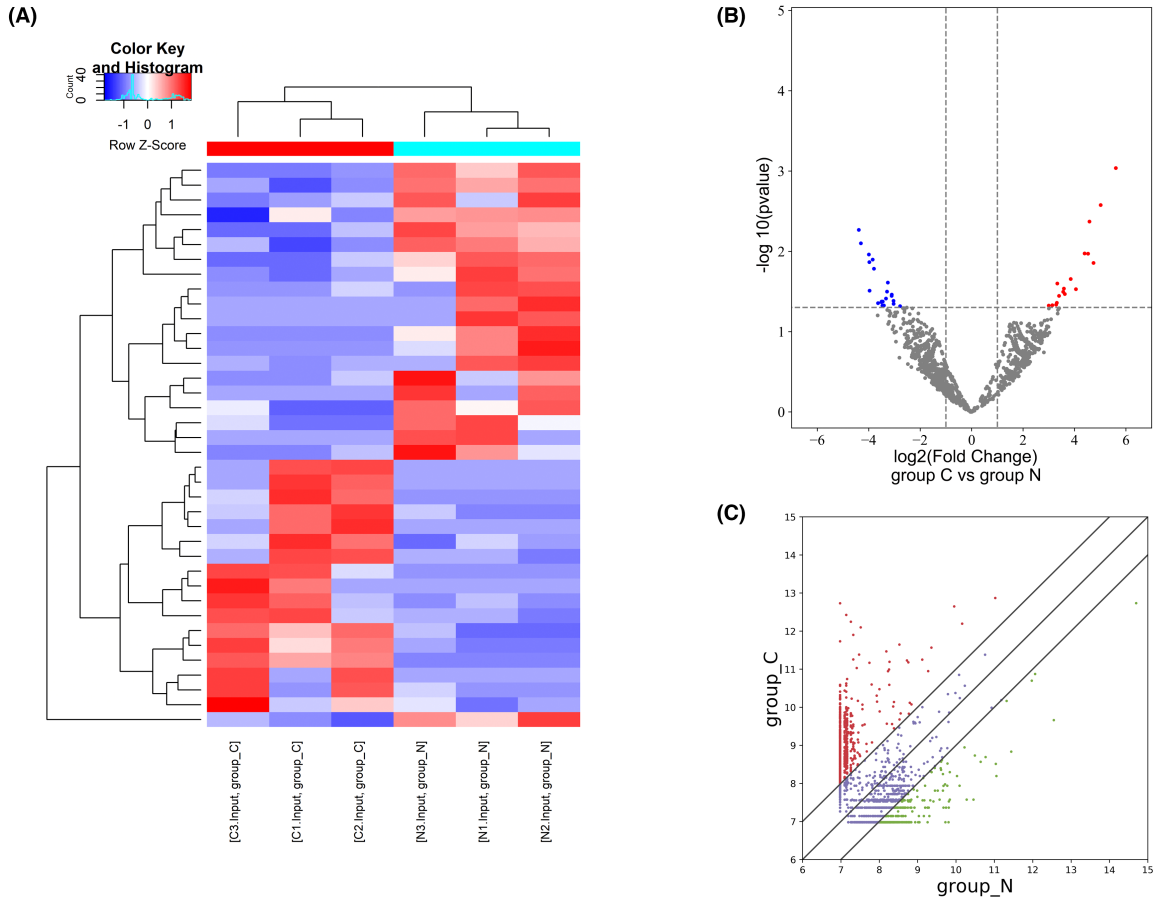
TABLE 4 Top 10 upregulated circRNAs in OSCC tissues.

CircRNA ID	logFC	p value	Regulation	chrom	GeneName
chr8:48192450-48206619+	5.607208389	0.000917717	Up	chr8	SPIDR
chr10:116590611-116608496+	5.017313526	0.002649356	Up	chr10	FAM160B1
chr17:28180406-28182248-	4.736787979	0.013949369	Up	chr17	SSH2
chr6:4891947-4892613+	4.581622734	0.004255499	Up	chr6	CDYL
chr1:85331068-85331821-	4.52738964	0.010705424	Up	chr1	LPAR3
chr1:117944808-117963271+	4.390161403	0.010629364	Up	chr1	MAN1A2
chr7:91924203-91957214+	4.057252902	0.029533416	Up	chr7	ANKIB1
chr14:21698478-21702388-	3.851118235	0.022127257	Up	chr14	HNRNPC
chr7:23015829-23023664-	3.62293183	0.034031938	Up	chr7	FAM126A
chr1:23356962-23377013+	3.587671322	0.029043577	Up	chr1	KDM1A

TABLE 5 Top 10 downregulated circRNAs in OSCC tissues.

CircRNA ID	logFC	p value	Regulation	chrom	GeneName
chr3:99567139-99569914-	−4.38792466	0.005397978	Down	chr3	FILIP1L
chr2:179516028-179516243-	−4.304194789	0.00794201	Down	chr2	TTN
chr2:24357989-24369956+	−3.997337247	0.010924474	Down	chr2	FAM228B
chr21:40578034-40584633-	−3.978976101	0.01362053	Down	chr21	BRWD1
chr5:65284463-65290692+	−3.967374591	0.030881657	Down	chr5	ERBB2IP
chrM:8469-8625+	−3.848112309	0.01266894	Down	chrM	OK/SW-cl.16
chr2:179517444-179517638-	−3.798906596	0.016457501	Down	chr2	TTN
chr6:170852689-170858201-	−3.639471148	0.044166724	Down	chr6	PSMB1
chrM:8928-9089+	−3.508243	0.042872255	Down	chrM	OK/SW-cl.16
chr18:56246046-56247780-	−3.501974296	0.042150597	Down	chr18	ALPK2

including the top five miRNAs that bind to the screened circRNAs and the top five mRNAs that bind to the miRNAs (Figure 7A). Furthermore, the network map included three differentially expressed circRNAs, 15 miRNAs, and 70 mRNAs. We used the circRNA (chr1:169947226-170001116, CircBase ID: hsa_circ_0111121) as an example and visualized its four hypermethylation sites (chr1:169974141-169974500, chr1: 169956461-169956900, chr1:169957121-169957340, chr1:169973641-169974020) using IGV software (v2.14.1; Figure 7B–E).

4 | DISCUSSION

Studies have shown that RNA modification can influence the development of human cancers.[46] Notably, numerous studies have shown the function of m7G methyltransferases in many cancers.[47] Methyltransferase-like1-WD repeat domain 4 (METTL1-WDR4) complex is known to be a methylase of m7G in tRNA, which plays an important role in various diseases.[48,49] In intrahepatic cholangiocarcinoma,[50] reduced METTL1 levels and aberrant m7G-modified tRNA levels may lead to ribosomal collisions, which selectively reduce translation efficiency. In HNSCC, the reduction in METTL1 reduces the m7G levels of 16 tRNAs, which prompts the development and progression of HNSCC.[28] To date, the major field of m7G epitranscriptome research focused on mRNA and tRNA m7G modification in cancer.[47] CircRNAs are important involved in the development of OSCC.[51] CircRNAs regulate the expression of their downstream genes by acting as miRNA sponge adsorbers.[52,53] Moreover, circRNAs modified with RNA methylation also emerge as important players in cancer. Ye et al. bridged the knowledge gaps between m6A modification and circRNAs fields by depicting the m6A-circRNAs genomic landscape and revealed the emerging roles played by m6A-circRNAs in pancreatic cancer.[54] He et al. analyzed the relationship between m6A modification and the expression and encoding potential of circRNAs in CRC.[55] In fact, many studies have reported the functional roles, cross-talk and clinical implications of m6A modification and circRNA.[56] The study from Zhao et al. utilized the data of MeRIP-seq and m6A-circRNAs epitranscriptomic microarray analysis to investigate the epitranscriptome-wide mapping of m6A-modified circRNA in OSCC.[57] However, more studies on the m7G modification of circRNAs are needed.
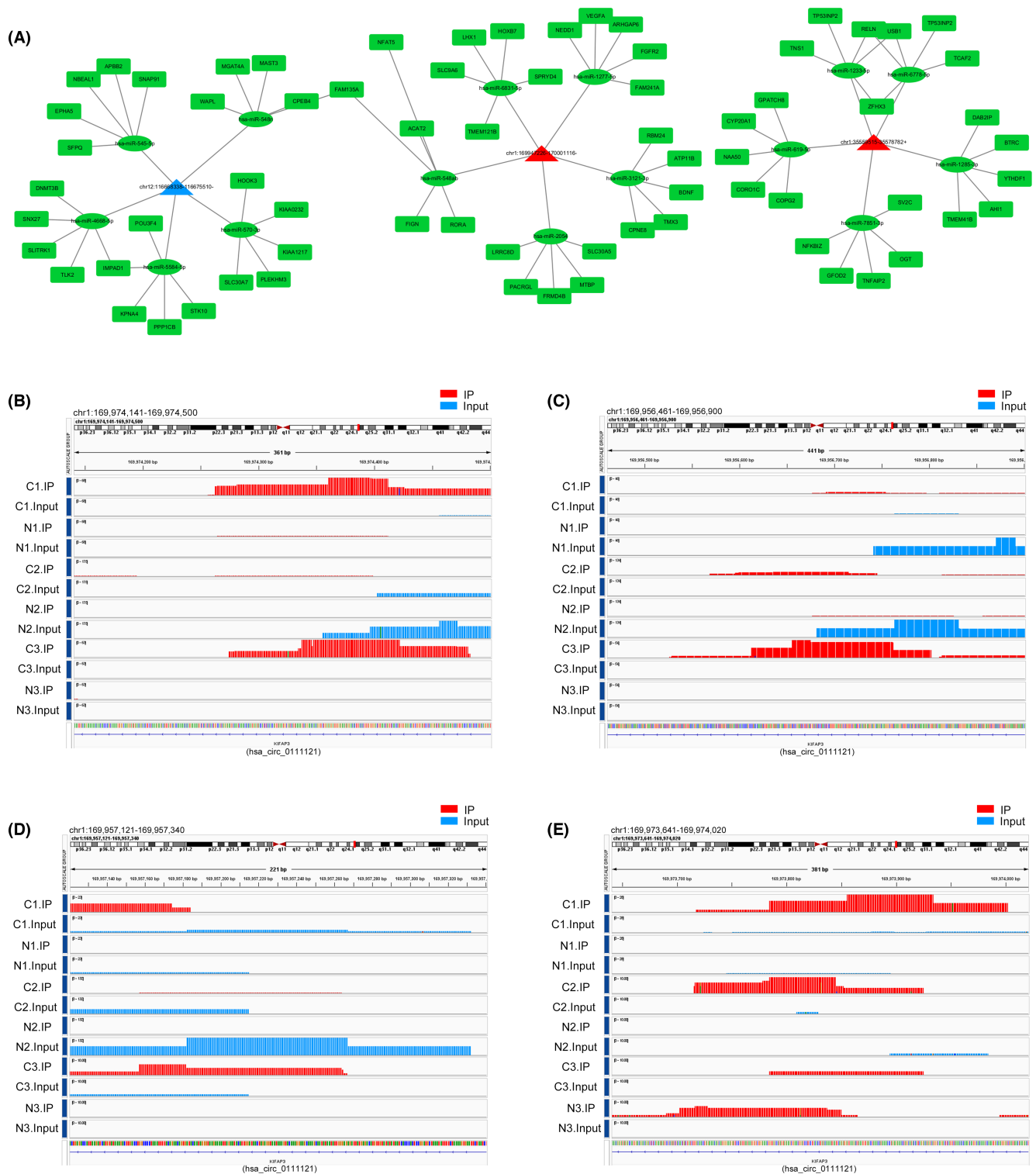
FIGURE 7 Co-analysis of m7G methylation and transcriptome in OSCC. (A) The circRNAs–miRNAs–mRNAs networks for hyper-methylated and hypo-methylated downregulated circRNAs. (B) Methylation peaks of circRNA "chr1:169947226-170001116" at the locus (Start: 169974141; End:169974500). (C) Methylation peaks of circRNA "chr1:169947226-170001116" at the locus (Start:169956461; End:169956900). (D) Methylation peaks of circRNA "chr1:169947226-170001116" at the locus (Start:169957121; End:169957340). (E) Methylation peaks of circRNA "chr1:169947226-170001116" at the locus (Start:169973641; End:169974020).

By sequencing OSCC tissues and normal tissues, we found a large difference in the number of m7G peaks and m7G-modified genes between OSCC and normal tissues.

Most m7G-modified circRNAs were derived from the sense overlapping region, followed by the exonic region. A relative decrease in the ratio of exonic-derived circRNAs with

m7G modification was observed. Interestingly, it has been reported that the reduced expression of exonic-derived circRNAs is associated with the mechanism of cancer development. A related study reported that circSMARCA5 can bind to its parent gene to form an R-loop, leading to transcriptional pauses at exon 15 of SMARCA5, which affects drug resistance in breast cancer.[58] We hypothesized that the reduction in exonic-derived circRNAs due to m7G methylation may affect the expression of some key regulators in OSCC, and the relevant mechanism needs further study.

GO enrichment and KEGG pathway analysis showed that differentially methylated and expressed genes were mainly enriched in antigen processing and presentation, cellular senescence and homologous recombination. Some of the biological functions and pathways were closely related to cancer. We observed that many genes were related to the immune response, which suggested that m7G-modified circRNAs were involved in the regulation of immune processes in OSCC. Previous studies have shown that cellular senescence and senescence-associated cytokines are major modulators in head and neck squamous cell carcinoma development.[59,60] He et al. found circRNAs implicated in OSCC carcinogenesis and progression through RNA sequencing and assessed differentially expressed circRNAs by GO and KEGG analysis.[61] In their study, genes were mainly enriched in cellular senescence, which was consistent with our results. Moreover, homologous recombination is known as a DNA repair pathway of clinical interest in cancer.[62] Studies have shown that proteins in homologous recombination pathways may be potential biomarkers in OSCC.[63] Therefore, the differentially methylated and expressed m7G-modified circRNAs and these pathways might provide clues for further research on the mechanism of OSCC. We analyzed the differentially expressed circRNAs to investigate the effect of differential m7G methylation on transcriptional expression. We identified hsa_circ_0111121, whose host gene is kinesin-associated protein 3 (KIFAP3). Studies have found that KIFAP3 is overexpressed in breast cancer.[64] Importantly, KIFAP3 regulates ciliary function important for Hedgehog signaling, and its mutation may induce the progression of basal cell carcinoma.[65] The relationship between m7G methylation modification and the expression level of hsa_circ_0111121 needs further study. We need to further explore the effect of m7G methylation on circRNA expression.

Our present study showed some correlation between circRNA expression and m7G methylation. In our study, to explore the effect of circRNA expression on genetic expression in OSCC, we constructed circRNA–miRNA–mRNA interaction networks. In the interaction network, we predicted 30 miRNAs interacting with six differentially expressed circRNAs and 142 target mRNAs of these miRNAs. Importantly, the study showed that the upregulated circRNA chr8:48192450-48206619 (CircBase ID: hsa_circ_0084188) derived from exonic region of SPIDR may bind to hsa-miR-1200 and thus affect the expression of hsa-miR-1200 target gene ubiquitin-like containing PHD and RING finger domains 1-binding protein 1 gene (UHRF1BP1). Furthermore, the levels of UHRF1BP1 were overexpression in HNSCC and associated with prognosis in patients with HPV-negative HNSCC.[66] We predicted that the upregulated circRNA chr8:48192450-48206619 could play a sponge adsorption role to upregulate UHRF1BP1 gene expression. From the network map, we found that circRNAs could act through sponge-adsorbed miRNAs, which also provides a potentially effective target for the treatment of OSCC.

In conclusion, our study revealed the profile of circRNA m7G methylation of OSCC, and circRNAs of differential m7G methylation and differential expression were identified. There were significant differences in the m7G methylation patterns of circRNAs between OSCC and normal tissues. Further bioinformatics analysis showed the biological significance of differentially methylated circRNAs and differentially expressed circRNAs, and the network maps of circRNA–miRNA–mRNA were constructed to find the key gene related to OSCC, which may provide a new sight for the diagnosis and treatment of OSCC.

AUTHOR CONTRIBUTIONS

YYJ designed the research. DYS, NS and MML contributed to the manuscript preparation. XC, XYZ and YY performed the data analysis. JCY, MQX, WTZ and HHJ performed the statistical analysis. CBH and HHJ collected the samples. All authors were involved in manuscript writing and approved the final manuscript.

ACKNOWLEDGMENTS

FUNDING INFORMATION

CONFLICT OF INTEREST STATEMENT
The authors declare that they have no competing interests.

DATA AVAILABILITY STATEMENT
The data presented in this study are available on request from the corresponding author. The datasets presented in this study have been deposited in the NCBI GEO database: GSE221398.

INSTITUTIONAL REVIEW BOARD STATEMENT
The study was conducted according to the guidelines of the Declaration of Helsinki, and approved by the Ethics Committee of Weifang Medical University (protocol code 2022YX007, date of approval 11.25.2021).

INFORMED CONSENT STATEMENT
Informed consent was obtained from all subjects involved in the study.

ORCID
Yingying Jiang https://orcid.org/0000-0001-9671-7548

REFERENCES

1. Ali J, Sabiha B, Jan HU, Haider SA, Khan AA, Ali SS. Genetic etiology of oral cancer. *Oral Oncol*. 2017;70:23-28.
2. Panzarella V, Pizzo G, Calvino F, Compilato D, Colella G, Campisi G. Diagnostic delay in oral squamous cell carcinoma: the role of cognitive and psychological variables. *Int J Oral Sci*. 2014;6:39-45.
3. Shahinas J, Hysi D. Methods and risk of bias in molecular marker prognosis studies in oral squamous cell carcinoma. *Oral Dis*. 2018;24:115-119.
4. Sung H, Ferlay J, Siegel RL, et al. Global cancer statistics 2020: GLOBOCAN estimates of incidence and mortality worldwide for 36 cancers in 185 countries. *CA Cancer J Clin*. 2021;71:209-249.
5. Manzano-Moreno FJ, Costela-Ruiz VJ, García-Recio E, Olmedo-Gaya MV, Ruiz C, Reyes-Botella C. Role of salivary MicroRNA and cytokines in the diagnosis and prognosis of oral squamous cell carcinoma. *Int J Mol Sci*. 2021;22:12215.
6. Adams BD, Parsons C, Walker L, Zhang WC, Slack FJ. Targeting noncoding RNAs in disease. *J Clin Invest*. 2017;127:761-771.
7. Kristensen LS, Andersen MS, Stagsted LVW, Ebbesen KK, Hansen TB, Kjems J. The biogenesis, biology and characterization of circular RNAs. *Nat Rev Genet*. 2019;20:675-691.
8. Luo J, Liu H, Luan S, Li Z. Guidance of circular RNAs to proteins' behavior as binding partners. *Cell Mol Life Sci*. 2019;76:4233-4243.
9. Nan A, Chen L, Zhang N, et al. Circular RNA circNOL10 inhibits lung cancer development by promoting SCLM1-mediated transcriptional regulation of the humanin polypeptide family. *Adv Sci*. 2019;6:1800654.
10. Liu J, Jiang X, Zou A, et al. circIGHG-induced epithelial-to-mesenchymal transition promotes oral squamous cell carcinoma progression via miR-142-5p/IGF2BP3 signaling. *Cancer Res*. 2021;81:344-355.
11. Zhao W, Cui Y, Liu L, et al. Splicing factor derived circular RNA circUHRF1 accelerates oral squamous cell carcinoma tumorigenesis via feedback loop. *Cell Death Differ*. 2020;27:919-933.
12. Xue C, Gu X, Bao Z, Su Y, Lu J, Li L. The mechanism underlying the ncRNA dysregulation pattern in hepatocellular carcinoma and its tumor microenvironment. *Front Immunol*. 2022;13:847728.
13. Slack FJ, Chinnaiyan AM. The role of non-coding RNAs in oncology. *Cell*. 2019;179:1033-1055.
14. Cheng Z, Yu C, Cui S, et al. circTP63 functions as a ceRNA to promote lung squamous cell carcinoma progression by upregulating FOXM1. *Nat Commun*. 2019;10:3200.
15. Dong W, Dai ZH, Liu FC, et al. The RNA-binding protein RBM3 promotes cell proliferation in hepatocellular carcinoma by regulating circular RNA SCD-circRNA 2 production. *EBioMedicine*. 2019;45:155-167.
16. Wang L, Yi J, Lu LY, et al. Estrogen-induced circRNA, circPGR, functions as a ceRNA to promote estrogen receptor-positive breast cancer cell growth by regulating cell cycle-related genes. *Theranostics*. 2021;11:1732-1752.
17. Chen L, Zhang S, Wu J, et al. circRNA_100290 plays a role in oral cancer by functioning as a sponge of the miR-29 family. *Oncogene*. 2017;36:4551-4561.
18. Peng QS, Cheng YN, Zhang WB, Fan H, Mao QH, Xu P. circRNA_0000140 suppresses oral squamous cell carcinoma growth and metastasis by targeting miR-31 to inhibit hippo signaling pathway. *Cell Death Dis*. 2020;11:112.
19. Yi C, Pan T. Cellular dynamics of RNA modification. *Acc Chem Res*. 2011;44:1380-1388.
20. Roundtree IA, Evans ME, Pan T, He C. Dynamic RNA modifications in gene expression regulation. *Cell*. 2017;169:1187-1200.
21. Wiener D, Schwartz S. The epitranscriptome beyond m(6)a. *Nat Rev Genet*. 2021;22:119-131.
22. Haag S, Kretschmer J, Bohnsack MT. WBSCR22/Merm1 is required for late nuclear pre-ribosomal RNA processing and mediates N7-methylation of G1639 in human 18S rRNA. *RNA*. 2015;21:180-187.
23. Yang S, Zhou J, Chen Z, et al. A novel m7G-related lncRNA risk model for predicting prognosis and evaluating the tumor immune microenvironment in colon carcinoma. *Front Oncol*. 2022;12:934928.
24. Zhang LS, Liu C, Ma H, et al. Transcriptome-wide mapping of internal N(7)-methylguanosine methylome in mammalian mRNA. *Mol Cell*. 2019;74:1304-1316.e1308.
25. Malbec L, Zhang T, Chen YS, et al. Dynamic methylome of internal mRNA N(7)-methylguanosine and its regulatory role in translation. *Cell Res*. 2019;29:927-941.
26. Xia X, Wang Y, Zheng JC. Internal m7G methylation: a novel epitranscriptomic contributor in brain development and diseases. *Mol Ther Nucleic Acids*. 2023;31:295-308.
27. Pandolfini L, Barbieri I, Bannister AJ, et al. METTL1 promotes let-7 MicroRNA processing via m7G methylation. *Mol Cell*. 2019;74:1278-1290.e1279.
28. Chen J, Li K, Chen J, et al. Aberrant translation regulated by METTL1/WDR4-mediated tRNA N7-methylguanosine modification drives head and neck squamous cell carcinoma progression. *Cancer Commun (Lond)*. 2022;42:223-244.

29. Zhang C, Cui H, Huang C, et al. Interactions of circRNAs with methylation: an important aspect of circRNA biogenesis and function. *Mol Med Rep*. 2022;25:169.

30. Chen Y, Lin H, Miao L, He J. Role of N7-methylguanosine (m(7)G) in cancer. *Trends Cell Biol*. 2022;32:819-824.

31. Kechin A, Boyarskikh U, Kel A, Filipenko M. cutPrimers: a new tool for accurate cutting of primers from reads of targeted next generation sequencing. *J Comput Biol*. 2017;24:1138-1143.

32. Dobin A, Davis CA, Schlesinger F, et al. STAR: ultrafast universal RNA-seq aligner. *Bioinformatics (Oxford, England)*. 2013;29:15-21.

33. Cheng J, Metge F, Dieterich C. Specific identification and quantification of circular RNAs from sequencing data. *Bioinformatics (Oxford, England)*. 2016;32:1094-1096.

34. Glažar P, Papavasileiou P, Rajewsky N. circBase: a database for circular RNAs. *RNA (New York, N.Y.)*. 2014;20:1666-1670.

35. Ghosal S, Das S, Sen R, Basak P, Chakrabarti J. Circ2Traits: a comprehensive database for circular RNA potentially associated with disease and traits. *Front Genet*. 2013;4:283.

36. Robinson MD, McCarthy DJ, Smyth GK. edgeR: a Bioconductor package for differential expression analysis of digital gene expression data. *Bioinformatics*. 2010;26:139-140.

37. Kim D, Langmead B, Salzberg SL. HISAT: a fast spliced aligner with low memory requirements. *Nat Methods*. 2015;12: 357-360.

38. Zhang Y, Liu T, Meyer CA, et al. Model-based analysis of ChIP-seq (MACS). *Genome Biol*. 2008;9:R137.

39. Shen L, Shao NY, Liu X, Maze I, Feng J, Nestler EJ. diffReps: detecting differential chromatin modification sites from ChIP-seq data with biological replicates. *PloS One*. 2013;8:e65598.

40. Qi X, Zhang DH, Wu N, Xiao JH, Wang X, Ma W. ceRNA in cancer: possible functions and clinical implications. *J Med Genet*. 2015;52:710-718.

41. Xu Y, Huang X, Ye W, et al. Comprehensive analysis of key genes associated with ceRNA networks in nasopharyngeal carcinoma based on bioinformatics analysis. *Cancer Cell Int*. 2020;20:408.

42. Enright AJ, John B, Gaul U, Tuschl T, Sander C, Marks DS. MicroRNA targets in drosophila. *Genome Biol*. 2003;5:R1.

43. Liu W, Wang X. Prediction of functional microRNA targets by integrative modeling of microRNA binding and target expression data. *Genome Biol*. 2019;20:18.

44. Otasek D, Morris JH, Bouças J, Pico AR, Demchak B. Cytoscape automation: empowering workflow-based network analysis. *Genome Biol*. 2019;20:185.

45. Bailey TL. DREME: motif discovery in transcription factor ChIP-seq data. *Bioinformatics*. 2011;27:1653-1659.

46. Yang B, Wang JQ, Tan Y, Yuan R, Chen ZS, Zou C. RNA methylation and cancer treatment. *Pharmacol Res*. 2021;174:105937.

47. Luo Y, Yao Y, Wu P, Zi X, Sun N, He J. The potential role of N(7)-methylguanosine (m7G) in cancer. *J Hematol Oncol*. 2022;15:63.

48. Li J, Wang L, Hahn Q, et al. Structural basis of regulated m(7)G tRNA modification by METTL1-WDR4. *Nature*. 2023;613:391-397.

49. Lin S, Liu Q, Lelyveld VS, Choe J, Szostak JW, Gregory RI. Mettl1/Wdr4-mediated m(7)G tRNA methylome is required for normal mRNA translation and embryonic stem cell self-renewal and differentiation. *Mol Cell*. 2018;71:244-255.e245.

50. Dai Z, Liu H, Liao J, et al. N(7)-Methylguanosine tRNA modification enhances oncogenic mRNA translation and promotes intrahepatic cholangiocarcinoma progression. *Mol Cell*. 2021;81:3339-3355.e3338.

51. Momen-Heravi F, Bala S. Emerging role of non-coding RNA in oral cancer. *Cell Signal*. 2018;42:134-143.

52. Hansen TB, Jensen TI, Clausen BH, et al. Natural RNA circles function as efficient microRNA sponges. *Nature*. 2013;495:384-388.

53. Liang ZZ, Guo C, Zou MM, Meng P, Zhang TT. circRNA-miRNA-mRNA regulatory network in human lung cancer: an update. *Cancer Cell Int*. 2020;20:173.

54. Ye Y, Feng W, Zhang J, et al. Genome-wide identification and characterization of circular RNA m(6)a modification in pancreatic cancer. *Genome Med*. 2021;13:183.

55. He F, Guo Q, Jiang GX, Zhou Y. Comprehensive analysis of m(6)a circRNAs identified in colorectal cancer by MeRIP sequencing. *Front Oncol*. 2022;12:927810.

56. Qin S, Mao Y, Chen X, Xiao J, Qin Y, Zhao L. The functional roles, cross-talk and clinical implications of m6A modification and circRNA in hepatocellular carcinoma. *Int J Biol Sci*. 2021;17:3059-3079.

57. Zhao, W., Liu, J., Wu, J., et al. High-throughput microarray reveals the epitranscriptome-wide landscape of m6A-modified circRNA in oral squamous cell carcinoma. *BMC Genomics.*. 2022;23:611.

58. Xu X, Zhang J, Tian Y, et al. CircRNA inhibits DNA damage repair by interacting with host gene. *Mol Cancer*. 2020;19:128.

59. Schoetz U, Klein D, Hess J, et al. Early senescence and production of senescence-associated cytokines are major determinants of radioresistance in head-and-neck squamous cell carcinoma. *Cell Death Dis*. 2021;12:1162.

60. Parkinson EK. Senescence as a modulator of oral squamous cell carcinoma development. *Oral Oncol*. 2010;46:840-853.

61. He Y, Yang D, Li Y, Xiang J, Wang L, Wang Y. Circular RNA-related CeRNA network and prognostic signature for patients with oral squamous cell carcinoma. *Front Pharmacol*. 2022;13:949713.

62. Hoppe MM, Sundar R, Tan DSP, Jeyasekharan AD. Biomarkers for homologous recombination deficiency in cancer. *J Natl Cancer Inst*. 2018;110:704-713.

63. Liu C, Liao K, Gross N, et al. Homologous recombination enhances radioresistance in hypopharyngeal cancer cell line by targeting DNA damage response. *Oral Oncol*. 2020;100:104469.

64. Telikicherla D, Maharudraiah J, Pawar H, et al. Overexpression of kinesin associated protein 3 (KIFAP3) in breast cancer. *J Proteomics Bioinformat*. 2012;5:122-126.

65. Onodera S, Morita N, Nakamura Y, et al. Novel alterations in IFT172 and KIFAP3 may induce basal cell carcinoma. *Orphanet J Rare Dis*. 2021;16:443.

66. El Baroudi M, Machiels JP, Schmitz S. Expression of SESN1, UHRF1BP1, and miR-377-3p as prognostic markers in mutated TP53 squamous cell carcinoma of the head and neck. *Cancer Biol Ther*. 2017;18:775-782.